PREPARED FOR THE U.S. DEPARTMENT OF ENERGY,
UNDER CONTRACT DE-AC02-76-CHO-3073

PPPL-2766
UC-427

PPPL-2766

A KINETIC-MHD MODEL FOR LOW FREQUENCY PHENOMENA

BY

C.Z. CHENG

July 1991

PRINCETON
PLASMA PHYSICS
LABORATORY

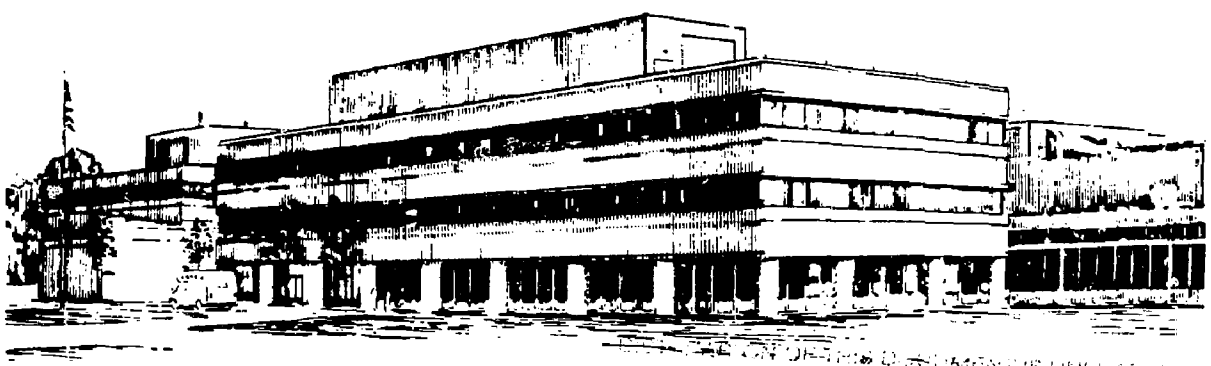

PRINCETON UNIVERSITY, PRINCETON, NEW JERSEY

NOTICE

This report was prepared as an account of work sponsored by an agency of the United States Government. Neither the United States Government nor any agency thereof, nor any of their employees, makes any warranty, express or implied, or assumes any legal liability or responsibility for the accuracy, completeness, or usefulness of any information, apparatus, product, or process disclosed, or represents that its use would not infringe privately owned rights. Reference herein to any specific commercial produce, process, or service by trade name, trademark, manufacturer, or otherwise, does not necessarily constitute or imply its endorsement, recommendation, or favoring by the United States Government or any agency thereof. The views and opinions of authors expressed herein do not necessarily state or reflect those of the United States Government or any agency thereof.

NOTICE

This report has been reproduced directly from the best available copy.

Available to DOE and DOE contractors from the:

Office of Scientific and Technical Information
P.O. Box 62
Oak Ridge, TN 37831;
Prices available from (615) 576-8401.

Available to the public from the:

National Technical Information Service
U.S. Department of Commerce
5285 Port Royal Road
Springfield, Virginia 22161
703-487-4650

A Kinetic-MHD Model for Low Frequency Phenomena

PPPL--2766

DE91 015378

C. Z. Cheng

Princeton Plasma Physics Laboratory
Princeton University, Princeton, NJ 08543

Abstract

A hybrid kinetic-MHD model for describing low-frequency phenomena in high beta ($\beta \sim O(1)$) anisotropic plasmas that consist of two components: a low energy core component and an energetic component with low density. The kinetic-MHD model treats the low energy core component by magnetohydrodynamic (MHD) description, the energetic component by kinetic approach such as the gyrokinetic equation, and the coupling between the dynamics of these two components through plasma pressure in the momentum equation. The kinetic-MHD model optimizes both the physics contents and the theoretical efforts in studying low frequency MHD waves and transport phenomena in general magnetic field geometries, and can be easily modified to include the core plasma kinetic effects if necessary. It is applicable to any magnetized collisionless plasma system where the parallel electric field effects are negligibly small. In the linearized limit two coupled eigenmode equations for describing the coupling between the transverse Alfvén type and the compressional Alfvén type waves are derived. The eigenmode equations are identical to those derived from the full gyrokinetic equation in the low frequency limit and were previously analyzed both analytically and numerically to obtain the eigenmode structure of the drift mirror instability [Cheng and Lin, 1987] which explains successfully the multi-satellite observation of antisymmetric field-aligned structure of the compressional magnetic field of Pc 5 waves [Takahashi et al., 1987] in the magnetospheric ring current plasma. Finally, a quadratic form is derived to demonstrate the stability of the low-frequency transverse and compressional Alfvén type instabilities in terms of the pressure anisotropy parameter τ and the magnetic field curvature-pressure gradient parameter α_p as defined in Eqs.(3.7) and (6.4), respectively. A procedure for determining the stability of a marginally stable MHD wave due to wave-particle resonances is also presented.

MASTER

1. Introduction

In space environment and large magnetic fusion devices the plasma can be considered to consist of two components of plasmas: the core component has low energy and satisfies magnetohydrodynamic (MHD) description, the energetic component has low density and MHD description is not valid for its dynamics. Typically, for the magnetospheric ring current plasma near the geosynchronous orbit the core plasma temperature is $T_c \approx 10 - 10^2$ eV, the hot plasma temperature is $T_h \approx 10^4$ eV, the ratio of the hot plasma to the core plasma density is $(n_h/n_c) \approx 10^{-1}$, and the ratio of core plasma beta to the hot plasma beta is $(\beta_c/\beta_h) \approx 10^{-2} - 10^{-1}$. For large tokamak devices, $T_c \approx 10^3 - 10^4$ eV, $T_h \approx 10^5 - 10^6$ eV, $(n_h/n_c) \approx 10^{-3} - 10^{-1}$, and $(\beta_c/\beta_h) \approx 1 - 10$. Instead of employing kinetic approach for all plasma components, a hybrid kinetic-MHD model is proposed to treat the low energy core component by MHD description, the energetic component by kinetic approach such as the gyrokinetic equation and Vlasov equation, and the coupling between the dynamics of these two components through plasma pressure in the momentum equation. The kinetic-MHD model optimizes both the physics contents and the theoretical efforts in studying low frequency phenomena. The kinetic-MHD model presented here also properly takes into account the dynamics of high-β ($\beta \sim O(1)$) plasma with pressure anisotropy in general magnetic field geometries and is useful in studying low frequency MHD type instabilities, wave propagation, and plasma transport. It should be noted that the applicability of the kinetic-MHD model presented here is not limited to the magnetospheric and tokamak plasmas; it is applicable to any magnetized collisionless plasma system where parallel electric field effects are negligibly small.

In the linearized limit, the kinetic-MHD model has been applied to study the effects of energetic particles on global MHD modes in tokamaks [Chen et al., 1984; Cheng, 1989, 1990a, 1991a, Cheng et al., 1990]. In the paper a set of two eigenmode equations is derived to describe the coupling between the transverse Alfvén type and the compressional Alfvén type waves in the limit that the perpendicular wavelength is small compared to the parallel wavelength and to the equilibrium scale length. These eigenmode equations are identical to those previously derived from the general frequency gyrokinetic equation for all particle species [Cheng and Lin,1987; Berk et al., 1983]; thus, the kinetic-MHD model contains the essential physics for low frequency phenomena. The transverse Alfvén wave equation shows that the shear Alfvén type waves can be strongly destabilized by the combined effect of the magnetic field curvature and the plasma pressure gradient to excite ballooning modes. The compressional Alfvén wave equation indicates that the drift mirror mode can be destabilized by the pressure anisotropy. The coupling between the compressional and transverse magnetic field is due to finite perpendicular pressure gradient and the trapped particle

perturbed pressures. The coupled eigenmode equations are particularly useful in studying low-frequency geomagnetic pulsations in the magnetosphere.

Geomagnetic pulsations in the magnetosphere are considered to be excited either by local field line resonances [Radoski, 1966; Cummings, 1969; Tataronis and Grossmann, 1973; Chen and Hasegawa, 1974; Southwood, 1974] in response to externally driven perturbations or by locally driven internal plasma instabilities [Hasegawa, 1969; Southwood, 1976; Pokhotelov et al., 1986; Cheng and Lin, 1987; Chen and Hasegawa, 1991]. The externally driven field line resonances in general have small azimuthal mode numbers on the order 10 or less and is observable on the ground. The internally driven plasma instabilities usually have large azimuthal mode numbers on the order of 100 and is mainly observed in the magnetosphere by satellites [Takahashi, 1988]. By solving the coupled eigenmode equations for the transverse and compressional waves both analytically and numerically, Cheng and Lin [1987] was the first to explain successfully the multi-satellite observation of antisymmetric field-aligned structure of the compressional magnetic field of Pc 5 waves [Takahashi et al., 1987] in the magnetospheric ring current region where the plasma perpendicular pressure is larger than the parallel pressure. Recently, Chen and Hasegawa [1991] proposed that the perturbed compressional magnetic field with antisymmetric field-aligned structure can be excited by the drift Alfvén ballooning mirror instability that requires lower pressure anisotropy threshold than the drift mirror instability. The drift Alfvén ballooning mirror instability is destabilized by hot particle pressure gradient via the magnetic drift-bounce resonance.

In Section 2 the kinetic-MHD model is presented. Three scalar equations are derived from the momentum equation to determine the dynamics of the slow magnetosonic waves, the shear Alfvén waves, and the fast magnetosonic waves, respectively. The validity of the kinetic-MHD model is also discussed. The anisotropic MHD equilibrium is discussed in Section 3. In Section 4 a set of linearized kinetic-MHD eigenmodes describing low-frequency transverse and compressional Alfvén instabilities is derived including the solution of the gyrokinetic equation. The eigenmode equations in the guiding center drift kinetic limit is given in Section 5. A quadratic form for describing the stability properties is presented in Section 6. Finally, a summary and conclusion is given in Section 7.

2. Kinetic-MHD Model

Let us consider a plasma consisting of a core (c) background component and a hot (h) component with the hot plasma density smaller than the core plasma density, $n_h << n_c$, and the hot

plasma temperature larger than the core plasma temperature, $T_h >> T_c$. In order to describe the low frequency MHD phenomena in such a plasma system we present a kinetic-MHD model. Since the plasma usually has anisotropic pressure in space environment and large magnetic fusion devices, we consider the momentum equation with anisotropic pressure

$$\rho \frac{d}{dt} \vec{V} = -\nabla \cdot \vec{\vec{p}} + \vec{j} \times \vec{b}, \tag{2.1}$$

where $(d/dt) = (\partial/\partial t) + \vec{V} \cdot \nabla$ is the total time derivative, $\vec{V}$ is the fluid velocity, $\vec{b}$ is the magnetic field, $\vec{\vec{p}}$ is the pressure tensor due to all particle species, and ρ is the total plasma mass density. The density continuity equation is given by

$$\frac{d}{dt} \rho + \rho \nabla \cdot \vec{V} = 0, \tag{2.2}$$

The following Maxwell's equations and ideal MHD relations hold:

the Faraday's law

$$\frac{\partial}{\partial t} \vec{b} = -\nabla \times \vec{E}, \tag{2.3}$$

the Ohm's law

$$\vec{E} + \vec{V} \times \vec{b} = 0, \tag{2.4}$$

the Ampere's law

$$\vec{j} = \nabla \times \vec{b}, \tag{2.5}$$

and

$$\nabla \cdot \vec{b} = 0, \tag{2.6}$$

where $\vec{E}$ is the electric field. The total plasma pressure $\vec{\vec{p}}$ can be expressed as

$$\vec{\vec{p}} = p_\perp \vec{\vec{I}} + (p_\parallel - p_\perp) \vec{b}\,\vec{b} / b^2, \tag{2.7}$$

where $p_{\parallel}$ and $p_{\perp}$ are the parallel and perpendicular pressures, respectively, and contain both the core and hot plasma pressures. To close Equations (2.1) - (2.7) we need to prescribe the pressure. Since the hot plasma density is much smaller than the core plasma density we shall employ the double-adiabatic pressure laws to relate the core plasma pressure to the plasma density;

$$\frac{d}{dt}\left(p_{\parallel c}\, p_{\perp c}^2 / \rho^5 \right) = 0 , \tag{2.8}$$

and

$$\frac{d}{dt}\left(p_{\perp c} / \rho b \right) = 0 . \tag{2.9}$$

For the hot component we will take into account the particle kinetic effects, such as finite Larmor radius and wave-particle resonances, by obtaining the parallel and perpendicular pressures from the hot particle distribution function f by

$$\begin{pmatrix} p_{\parallel h} \\ p_{\perp h} \end{pmatrix} = \sum_j m_j \int d^3v\, f_j \begin{pmatrix} v_{\parallel}^2 \\ v_{\perp}^2/2 \end{pmatrix} , \tag{2.10}$$

where the summation in j is over all hot particle species, m is the particle mass, and $v_{\parallel}$ and $v_{\perp}$ are the particle velocity parallel and perpendicular to the magnetic field $\vec{b}$, respectively.

The low-frequency gyrokinetic formulation is employed to describe the dynamics of all hot particle species. We write $f = F + \delta f$, and $\vec{b} = \vec{B} + \delta\vec{B}$, where F and $\vec{B}$ are the unperturbed particle distribution function and magnetic field, respectively, and δf and $\delta\vec{B}$ are the perturbed particle distribution function and magnetic field, respectively. We will consider low-frequency waves (wave frequency is smaller than the ion cyclotron frequency) with perpendicular wavelength small compared to the parallel wavelength and to the equilibrium scale length. A WKB eikonal representation is adopted for the perturbed quantities, i.e.,

$$\delta f(\vec{x}, \vec{v}, t) = \delta f(s, \vec{k}_{\perp}, \vec{v}, t)\, \exp\left[i \int d\vec{x}_{\perp} \cdot \vec{k}_{\perp} \right] , \tag{2.11}$$

where s is the distance along the equilibrium magnetic field, and $\vec{k}_\perp$ is the perpendicular wave vector. The nonlinear gyrokinetic equation is expressed in terms of the guiding center variables, the particle energy $\varepsilon = v^2/2$, the magnetic moment $\mu = v_\perp^2/2B$, and gyrophase angle, where v is the particle velocity and $v_\perp$ is the particle velocity perpendicular to the equilibrium magnetic field. Note that implicitly assumed in the gyrokinetic formalism is that $\delta f << F$ and $\delta\vec{B} << \vec{B}$ so that $v_\parallel$ and $v_\perp$ differ from those needed in computing the pressure from Eq.(2.10) by an order of $|\delta\vec{B}/\vec{B}|$. The perturbed particle distribution function δf for a given species is written as

$$\delta f = \frac{e}{m}\frac{\partial F}{\partial \varepsilon}\phi + \frac{e}{mB}\frac{\partial F}{\partial \mu}\left(\phi - \frac{v_\parallel A_\parallel}{c}\right) + \left[g - \frac{e}{mB}\frac{\partial F}{\partial \mu}\langle \delta L\rangle\right]\exp(iL_0)\,, \tag{2.12}$$

where

$$\langle \delta L\rangle = \left(\phi - \frac{v_\parallel A_\parallel}{c}\right) J_0\left(\frac{k_\perp v_\perp}{\omega_c}\right) + \frac{v_\perp \delta B_\parallel}{c\,k_\perp} J_1\left(\frac{k_\perp v_\perp}{\omega_c}\right)\,, \tag{2.13}$$

$$L_0 = \frac{\vec{k}_\perp \times \vec{v}_\perp \cdot \vec{B}}{\omega_c B}\,. \tag{2.14}$$

Note that $v_\parallel$, $A_\parallel$, and $\delta B_\parallel$ are the particle velocity, vector potential, and perturbed magnetic field parallel to the equilibrium magnetic field $\vec{B}$, respectively. J_0 and J_1 are the Bessel function of order 0 and 1, respectively, e is the particle charge, $\omega_c = eB/mc$ is the cyclotron frequency, ϕ is the electrostatic potential. The nonadiabatic particle distribution g is governed by the nonlinear gyrokinetic equation [Frieman and Chen, 1982] by

$$\left[\frac{\partial}{\partial t} + (\vec{v}_\parallel + \vec{v}_d)\cdot\nabla\right] g = -\left[\frac{e}{m}\frac{\partial F}{\partial \varepsilon}\frac{\partial}{\partial t} - \frac{c\,\vec{B}\times\nabla F}{B^2}\cdot\nabla\right]\langle \delta L\rangle$$

$$- \frac{c}{B^2}\nabla g \cdot \vec{B}\times\nabla\langle \delta L\rangle\,, \tag{2.15}$$

where $\vec{v}_d = (\vec{B}/B\omega_c) \times [\,\nabla(\mu B) + \vec{\kappa}\, v_\parallel^2]$ is the particle magnetic drift velocity in the equilibrium magnetic field, $\vec{\kappa} = (\vec{B}/B)\cdot\nabla(\vec{B}/B)$ is the equilibrium magnetic field curvature. Equation (2.15)

shows that the nonlinearity arises from a gyrophase-averaged effective $\vec{E}_{eff}\times\vec{B}\bullet\nabla$ coupling, where $\vec{E}_{eff} = -\nabla(\phi - \vec{v}\bullet\vec{A}/c)$. Note that the nonlinear polarization drift is contained within the finite Larmor radius corrections in J_0 and J_1. The electric field is related to the electrostatic potential and the vector potential $\vec{A}$ by $\vec{E} = -\nabla\phi + (1/c)\,\partial\vec{A}/\partial t$, where $\delta\vec{B} = \nabla\times\vec{A}$.

There are improved gyrokinetic formalisms that include small corrections to Eq.(2.15) to conserve phase space volume [Hahm, 1988; Brizard, 1989]. The nonlinear gyrokinetic equation can be either directly integrated in the five-dimensional phase space [Tsang and Cheng, 1991] or simulated by a gyrokinetic particle simulation technique [Lee, 1987]. It is important to mention that a particle simulation [Cheng and Okuda, 1977a] of electron dynamics governed by the drift kinetic equation and ion dynamics governed by the Vlasov equation was developed to study low-frequency drift waves and trapped particle instabilities and the corresponding plasma transport in the complex toroidal geometry [Cheng and Okuda, 1977b, 1978a, 1978b]. Numerical integration of Vlasov equation in six-dimensional phase space was also studied by Cheng [1977]. Three-dimensional MHD simulations for the magnetosphere and tokamaks have been developed for years. Thus, the kinetic-MHD model presented here should be able to be studied by these previously developed techniques with the present day computing power.

Equations (2.1)-(2.15) form the basis of the kinetic-MHD model for studying low-frequency phenomena. In the guiding center limit where $(k_\perp v_\perp/\omega_c) << 1$ (the particle gyroradius is very small compared to the perpendicular wavelength), the Bessel functions J_0 and J_1 can be expanded to the lowest order, and we have

$$\langle\delta L\rangle = \phi - v_\parallel A_\parallel/c + m\mu\,\delta B_\parallel/e\,. \qquad (2.16)$$

The WKB ansatz, Eq.(2.11), employed for the finite Larmor radius gyrokinetic formulation is no longer relevant, and the guiding center drift kinetic-MHD model should be applicable to low-frequency waves with perpendicular wavelength comparable to the parallel wavelength and the equilibrium scale length. When more accurate solution of δf is required, such as in the magnetotail region where the particle Larmor radius is comparable to the equilibrium scale length, the Vlasov equation can be employed to solve δf in order to couple to the MHD fluid equations.

It is important to note that when the kinetic effects of the core plasma component such as wave-particle resonance must be included, the double-adiabatic pressure law should be replaced by the gyrokinetic description, i.e., the core component can be treated similarly as the hot component.

This approach still has the advantage over the fully kinetic description for all species because in the kinetic-MHD model the kinetic description couples to the MHD description only through the particle pressure. Therefore, the kinetic-MHD model is applicable to any magnetized collisionless plasma system where parallel electric field due to kinetic effects can be neglected. We also note that the kinetic-MHD model can be trivially extended to include the plasma resistivity effect and finite electron inertia by using the modified Ohm's law.

The momentum equation, Eq.(2.1), is a very complicated vector equation and can be written into more useful forms given by

$$\rho \frac{d}{dt} \vec{V} = \sigma \vec{j} \times \vec{b} - \nabla P_\perp + (\sigma - 1) \nabla(b^2/2) + \vec{b}\ \vec{b} \cdot \nabla \sigma$$
$$= -\nabla(P_\perp + b^2/2) + \sigma \vec{b} \cdot \nabla \vec{b} + \vec{b}\ \vec{b} \cdot \nabla \sigma , \qquad (2.17)$$

where

$$\sigma = 1 + (P_\perp - P_\parallel) / b^2. \qquad (2.18)$$

Equation (2.17) can be cast into three scalar equations that describe the dynamics of the slow magnetosonic waves, the shear Alfvén waves, and the fast magnetosonic waves, respectively. The projection along the magnetic field yields information on parallel momentum balance

$$\rho \vec{b} \cdot \frac{d}{dt} \vec{V} = -\vec{b} \cdot \nabla P_\parallel + (P_\parallel - P_\perp) \vec{b} \cdot \nabla b / b , \qquad (2.19)$$

which describes the propagation of the slow magnetosonic waves. From Eq.(2.17), we see that $\nabla (P_\perp + b^2/2)$ is the dominant term. The other two scalar equations should be the ones with and without the $\nabla(P_\perp + b^2/2)$ information, respectively. An appropriate annihilation operator to eliminate the $\nabla(P_\perp + b^2/2)$ term is $\vec{b} \cdot \nabla \times$ which is applied to Eq.(2.17). With this operation we obtain the parallel current equation, which represents the vanishing of the divergence of the current and describes mainly the transverse Alfvén waves,

$$\nabla \cdot (\rho \vec{b} \times \frac{d}{dt} \vec{V}) + b^2 \vec{b} \cdot \nabla \left(\frac{\sigma \vec{j} \cdot \vec{b}}{b^2}\right) - \vec{b} \times \left[\left(\frac{\vec{b}}{b}\right) \cdot \nabla \left(\frac{\vec{b}}{b}\right)\right] \cdot \nabla (b^2/2 - P_\parallel)$$

$$+ \rho \frac{d}{dt}\vec{V} \bullet (\frac{\vec{b} \times \nabla b}{b}) - (\rho \vec{b} \bullet \frac{d}{dt}\vec{V}) (\frac{\vec{j} \bullet \vec{b}}{b^2}) = 0 . \qquad (2.20)$$

To retain the $\nabla(P_\perp + b^2/2)$ information, we apply the $\vec{b}\bullet\nabla\times\vec{b}\times$ operator to the momentum equation. Since the $\vec{b}\times$ operator removes the parallel information, we obtain the perpendicular current equation, which describes mainly the fast magnetosonic (compressional Alfvén) waves,

$$\begin{aligned}
&\vec{b} \bullet \nabla \times (\rho \vec{b} \times \frac{d}{dt}\vec{V}) + b^2 \nabla^2 (P_\perp + b^2/2) - \vec{b} \bullet \nabla [\vec{b} \bullet \nabla (P_\perp + b^2/2)] \\
&\quad + \vec{b} \bullet \nabla [\sigma \vec{b} \bullet \nabla (b^2/2)] + \sigma b^2 [\vec{b} \bullet \nabla^2 \vec{b} - \nabla^2 (b^2/2)] \\
&\quad + (\nabla b^2 + \vec{j} \times \vec{b}) \bullet \nabla (P_\perp + b^2/2) - [\nabla (b^2/2) + \vec{j} \times \vec{b}] \bullet \nabla (\sigma b^2) \\
&\quad - \sigma (\vec{j} \times \vec{b}) \bullet \nabla (b^2/2) + \sigma (\vec{j} \bullet \vec{b})^2 = 0 .
\end{aligned} \qquad (2.21)$$

Equations (2.1)-(2.21) constitute a nonlinear kinetic-MHD model for describing low frequency MHD type phenomena in a plasma with anisotropic pressure. The detailed derivation of Eqs. (2.19)-(2.21) is given in Appendix A. The kinetic-MHD model not only singles out the dominant physics of the core and energetic component plasmas but also greatly simplifies the theoretical efforts of studying the low-frequency MHD type phenomena. We note that these three scalar momentum equation presented above are very useful for both analytical analysis and numerical solutions the dominant physics are singled in certain terms. In particular, when the contribution from the fast magnetosonic wave can be ignored, a numerical implicit scheme can be applied to the $\nabla^2(P_\perp + b^2/2)$ term so that low frequency phenomena associated with the transverse Alfvén waves can be simulated in a longer physical time by large time steps.

It is important to discuss the validity of the kinetic-MHD model for collisionless plasma. The weakest approximation of the kinetic-MHD model is in the Ohm's law, which assumes that the parallel electric field vanishes. Physically, the vanishing parallel electric field assumed in the Ohm's law represents the assumption of negligibly small particle Larmor radius effects. This can be seen from the quasi-neutrality condition by summing the perturbed particle densities obtained from the linearized gyrokinetic equation [Berk et al., 1983];

$$\sum_j e \int d^3v \left\{ \frac{e}{m} \frac{\partial F}{\partial \varepsilon} J_o^2 (\chi - \phi) - (\frac{e}{m} \frac{\partial F}{\partial \varepsilon} + \frac{e}{mB} \frac{\partial F}{\partial \mu}) (1 - J_o^2) \phi \right.$$

$$+ \frac{c}{\omega B^2}\vec{k}_\perp \bullet \vec{B}\times\nabla F\, J_0{}^2\chi + \frac{e}{mB}\frac{\partial F}{\partial \mu} J_0 J_1 \frac{v_\perp \delta B_{\parallel}}{c\, k_\perp} - \tilde{g} J_0 \Big\} = 0 , \qquad (2.22)$$

where the summation is over all particle species j, $\vec{B}\bullet\nabla\chi = i\omega A_{\parallel}/cB$, and $\tilde{g}$ is the nonadiabatic particle distribution. In general, $\tilde{g}$ is expressed in integral forms and is shown in Section 4. In two limits, (1) high bounce frequency [$\omega_b >>$ max (ω,ω_d)] and (2) low bounce frequency [$\omega_b <<$ max (ω,ω_d)], $\tilde{g}$ is roughly given by [Berk et al., 1983]

$$\tilde{g} = \frac{eF}{T}\frac{(\tilde{\omega}-\omega_*^T)}{(\omega - <\omega_d>)} <J_0(\phi-\chi) + \frac{\omega_d}{\omega} J_0\chi + J_1\frac{v_\perp \delta B_{\parallel}}{c\, k_\perp}> , \qquad (2.23)$$

where ω_b is the bounce frequency, $\omega_d = \vec{k}_\perp \bullet \vec{v}_d$ is the magnetic drift frequency, T is the temperature, $\omega_*^T = \frac{cT}{eB^2}\vec{k}_\perp \bullet \vec{B}\times\nabla \ln F$, and $\tilde{\omega} = -\omega\frac{\Gamma}{m}\frac{\partial \ln F}{\partial \varepsilon}$. Here we use the <X> symbol in both the high and low bounce frequency regimes by defining that <X> = X when $\omega_b <<$ max (ω,ω_d), and <X> means the bounce average of X when $\omega_b >>$ max (ω,ω_d). Since $E_{\parallel} = -\vec{B}\bullet\nabla(\phi - \chi)$, the ideal MHD approximation $E_{\parallel} \approx 0$ is valid when the particle species sum over terms containing $(\phi - \chi)$ is dominant over other contributions. In the small Larmor radius limit, i.e. $(k_\perp v_\perp/\omega_c) < 1$, and including the leading order finite Larmor radius effect, the quasi-neutrality condition reduces to

$$(\chi-\phi) = \sum_j \Big\{\frac{ne^2}{T}\Big[\frac{k_\perp^2 T}{m\,\omega_c^2}\phi + \frac{\omega_{*\perp}}{\omega}\frac{k_\perp^2 P_\perp}{n\,m\,\omega_c^2}\chi - \frac{B}{n}\Big(\frac{\partial n}{\partial E}\Big)_\psi \frac{T\,\delta B_{\parallel}}{e\,B}\Big]$$

$$- \int d^3v \frac{e^2 F}{T}\frac{(\tilde{\omega}-\omega_*^T)}{(\omega - <\omega_d>)} <(\phi-\chi) + \frac{\omega_d}{\omega}\chi + \frac{m\,v_\perp^2\,\delta B_{\parallel}}{e\,B}>\Big\} \Big/ \sum_j \Big(\frac{ne^2}{T}\Big) , \qquad (2.24)$$

where $\omega_{*\perp} = \frac{cT}{eB^2}\vec{k}_\perp \bullet \vec{B}\times\tilde{\nabla}\ln(P_\perp)$, $\tilde{\nabla} = \nabla - \nabla B\,(\partial/\partial B)_\psi$, n is the particle density, $P_\perp$ is the perpendicular pressure, and ψ is the magnetic flux function. Therefore, the ideal MHD approximation $E_{\parallel} \approx 0$ is valid if the right hand-side of Eq.(2.24) is small. If for each particle

species ($nZ^2\omega_d/T\omega$), ($nZ^2\omega_{*\perp}/T\omega$), and $nZ^2[\partial\ln(n)/\partial\ln(B)]_\psi/T$ are smaller than $\sum_j (nZ^2/T)$, where Z is the particle charge state, $E_\parallel \approx 0$ holds even if the perturbation is dominantly a compressional Alfvén wave.

For the ring current plasma near the geosynchronous orbit, typically the core plasma temperature is $T_c \approx 10 - 10^2$ eV, the hot plasma temperature is $T_h \approx 10^4$ eV, the ratio of the hot plasma density to the core plasma density is $(n_h/n_c) \approx 10^{-1}$, thus the ratio of core plasma beta to the hot plasma beta is $(\beta_c/\beta_h) \approx 10^{-2} - 10^{-1}$. The hot proton gyroradius ρ is approximately 100 km, the azimuthal wave number is $M \approx 10^2$, thus $(k_\perp\rho)^2 \approx (2.5 \times 10^{-3}M)^2 = 0.0625 << 1$. The ion cyclotron frequency is $\omega_{ci} \approx 15\ s^{-1}$, the hot proton bounce frequency is $\omega_b \approx 4 \times 10^{-2}\ s^{-1}$, and the bounce averaged hot proton magnetic drift frequency is $\langle\omega_d\rangle \approx 10^{-4}M\ s^{-1}$. The hot proton pressure scale length is approximately 1 R_E, so that its diamagnetic drift frequency is $\omega_* \approx 4 \times 10^{-4}M\ s^{-1}$. For low frequency waves (eg. Pc 5 waves) with $\omega \approx 10^{-2}\ s^{-1}$, we have $(\omega/\omega_b) < 1$. Therefore, from Eq.(2.24) the ideal MHD approximation $E_\parallel \approx 0$ is justified. Note that since $(n_h/n_c) << 1$, $E_\parallel \approx 0$ can still be valid even if $\omega - \langle\omega_d\rangle - \omega_b \approx 0$ resonance occurs for the hot protons.

3. Anisotropic MHD Equilibrium

For a general three dimensional magnetospheric or toroidal equilibrium with nested flux surfaces, the magnetic field can be expressed as

$$\vec{B} = \nabla\psi \times \nabla\alpha\ , \tag{3.1}$$

where ψ is chosen as the magnetic flux function. Both ψ and α are constant along magnetic field lines. The lines where surfaces of constant ψ and α intersect represent magnetic field lines. Note that ψ must be a periodic function of toroidal angle ϕ in cylindrical (R, ϕ, Z) coordinate to ensure periodicity constraint. In terms of a flux coordinate system (ψ,Θ,ϕ) with Θ is the generalized poloidal angle varying between 0 and 2π, α can be expressed as $\alpha = \phi - q(\psi)\Theta - \Delta(\psi,\Theta,\phi)$ without loss of generality, where $\Delta(\psi,\Theta,\phi)$ is periodic in both Θ and ϕ. The flux coordinate system is in general not orthogonal and its metric is complicated because $\nabla\psi \bullet \nabla\Theta \neq 0$, $\nabla\psi \bullet \nabla\phi \neq 0$, and $\nabla\phi \bullet \nabla\Theta \neq 0$. A straight field line flux coordinate can be constructed by choosing $\zeta = \phi$

$-\Delta(\psi,\Theta,\phi)$ to replace ϕ so that $\vec{B}\bullet\nabla\zeta / \vec{B}\bullet\nabla\Theta = q(\psi)$. This feature is particularly useful since the operator $\vec{B}\bullet\nabla$ occurs frequently in the stability calculations.

If the plasma convection is small, the magnetospheric equilibrium can be approximated by a static MHD equilibrium. Let $\vec{J}$, $P_\perp$ and $P_\parallel$ be the equilibrium current, perpendicular and parallel pressures, respectively. $P_\perp$ and $P_\parallel$ are functions of magnetic flux function ψ and the magnitude of the magnetic field B. From Eq. (2.15), the momentum balance equation parallel to the equilibrium magnetic field is given by

$$\vec{B} \bullet \nabla P_\parallel = (P_\parallel - P_\perp) \vec{B}\bullet \nabla B / B , \tag{3.2}$$

and from Eq.(2.13), the momentum balance equation perpendicular to the magnetic field is given by

$$\nabla_\perp (B^2 / 2 + P_\perp) = \vec{\kappa}\, \sigma B^2 , \tag{3.3}$$

where σ can be expressed as

$$\sigma = 1 - (1/B)(\partial P_\parallel/\partial B)_\psi = 1 + (P_\perp - P_\parallel) / B^2. \tag{3.4}$$

For a simplified axisymmetric magnetospheric equilibrium with nested flux surfaces, the magnetic field can be expressed as

$$\vec{B} = \nabla\psi \times \nabla\phi . \tag{3.5}$$

where ψ is a function of R and Z only. Since $\vec{B}\bullet\nabla\psi = \vec{B}\bullet\nabla\phi = 0$, the lines of the magnetic field and the lines of constant ψ coincide. The $\nabla\phi$ component of Eq. (2.13) gives $\vec{J}\bullet\nabla\psi = 0$. The $\nabla\psi$ component of Eq. (2.13) leads to the toroidal ring current density

$$J_\phi = (R/\sigma) [(\partial P_\perp/\partial\psi)_B + (\tau - \sigma) (\nabla\psi\bullet\nabla B^2) / 2(\nabla\psi)^2] , \tag{3.6}$$

where the pressure anisotropy parameter τ is given by

$$\tau \cong 1 + (1/B)(\partial P_\perp/\partial B)_\psi . \tag{3.7}$$

Since $\vec{J} \bullet \nabla\phi = \nabla \bullet (\vec{B} \times \nabla\psi) = -\nabla \bullet (\nabla\psi/R^2)$, and

$$\nabla\psi \bullet \nabla\sigma = (\nabla\psi)^2 [\partial(P_\perp - P_\parallel)/\partial\psi]_B / B^2 + (\tau - \sigma)(\nabla\psi \bullet \nabla B^2) / 2B^2, \qquad (3.8)$$

the anisotropic equilibrium equation [Grad, 1967] for axisymmetric equilibrium can be written in the familiar form

$$R^2 \nabla \bullet (\nabla\psi / R^2) = -(1/\sigma) [R^2 (\partial P_\parallel/\partial\psi)_B + \nabla\psi \bullet \nabla\sigma], \qquad (3.9)$$

which will be used to solve for ψ if the functional form of $P_\parallel(\psi,B)$ and appropriate boundary conditions are specified. Extensive numerical solutions of Eq. (3.9) have been performed [Cheng, 1991b]. The isotropic limit of Equation (3.9) is obtained by setting $P_\perp = P_\parallel$, so that $\sigma = 1$. In the vacuum case, the right hand side of Eq. (3.9) is identically zero. One of the vacuum solution is the dipole field with $\psi = -M \sin^2\theta / r$, where r and θ are the radius and polar angle in the spherical coordinate system (r,θ,ϕ), and M is the dipole moment. The components of the dipole magnetic field are given by $B_r = -2M \cos\theta / r^3$, and $B_\theta = -M \sin\theta / r^3$. Another vacuum solution is the uniform interplanetary magnetic field (IMF) along the Z-axis with $\psi = B_{IMF} R^2 / 2$, where B_{IMF} is the constant IMF.

It is important to consider the effect of pressure anisotropy to the magnetospheric ring current. Typically, both $(\tau - \sigma)$ and $[(\nabla\psi \bullet \nabla B^2) / (\nabla\psi)^2]$ are negative and decrease in magnitude along the field lines as one moves away from the equator. For example, $(\nabla\psi \bullet \nabla B^2) / (\nabla\psi)^2 = -6M (1 + \cos^2\theta) / r^5(1 + 3\cos^2\theta) < 0$ for a dipole field, and $(\tau - \sigma) = -(2P_\perp + P_\parallel)(P_\perp/P_\parallel - 1) / B^2 < 0$ for a bi-Maxwellian distribution. Since $(\tau - \sigma)$ decreases in magnitude faster than $[(\nabla\psi \bullet \nabla B^2) / (\nabla\psi)^2]$ along the field line away from the equator, from Eq.(3.6) one expects that pressure anisotropy contributes to an eastward current which is peaked at the equator, and the westward ring current can be peaked away from the equator due to this anisotropic pressure driven eastward ring current.

In solving the equilibrium equation we specify $\vec{P}$ by prescribing the particle guiding center distribution for each species. For a collisionless plasma the particle energy ($\varepsilon = v^2/2$) and the adiabatic invariants, magnetic moment ($\mu = v_\perp^2 / 2B$) and the longitudinal invariant ($J_\parallel = \int ds\, v_\parallel$), are constant during the drift motions, where $v_\parallel$ and $v_\perp$ are the components of the velocity parallel and perpendicular to $\vec{B}$ respectively. The guiding center particle distribution function must have the

form $F = F(\varepsilon,\mu,J_\parallel)$. In general, $J_\parallel = J_\parallel(\varepsilon,\mu,\psi,\alpha)$ and $F = F(\varepsilon,\mu,\psi,\alpha)$, where ψ and α are related to the magnetic field through Eq.(3.1). If all particles on each field line share the same drift surface, where ψ labels the drift surface, then $J_\parallel = J_\parallel(\varepsilon,\mu,\psi)$ and $F = F(\varepsilon,\mu,J_\parallel)$. With this form of particle distribution, the parallel and perpendicular pressures are given by

$$\begin{pmatrix} P_\parallel \\ P_\perp \end{pmatrix} = \sum_{j,\sigma_\parallel} 2\pi m_j \int_0^\infty d\varepsilon \int_0^{\varepsilon/B} d\mu \, [\, B F_j / |v_\parallel| \,] \begin{pmatrix} 2(\varepsilon - \mu B) \\ \mu B \end{pmatrix}, \tag{3.10}$$

where the summation is over the particle species j and $\sigma_\parallel$ which represents the direction of particle velocity parallel to $\vec{B}$, and m_j is the particle mass. The parallel velocity $v_\parallel$ has the form $v_\parallel = \sigma_\parallel \sqrt{2(\varepsilon - \mu B)}$. By inspection $P_\perp$ and $P_\parallel$ are functions of ψ and B only. Note that the parallel pressure balance equation, Eq. (3.3), is automatically satisfied if the particle distribution $F(\varepsilon,\mu,\psi)$ is used to compute $P_\perp$ and $P_\parallel$. The guiding-center particle distributions $F(\varepsilon,\mu,\psi)$ can be either prescribed by an analytical form or obtained from the satellite measurements of the particle flux. The particle density and pressure everywhere along field lines can be integrated from an analytical distribution. For a bi-Maxwellian particle distribution $F(\varepsilon,\mu,\psi) = N(\psi)\,[2\pi T_\parallel(\psi)/m]^{-3/2} \exp[-m\varepsilon/T_\parallel(\psi) + m\mu B_o(\psi)/T_o(\psi)]$, the particle density is given by $n(\psi,B) = N(\psi)\,[T_\perp(\psi,B) / T_\parallel(\psi)] = N(\psi)\,[\,1 - B_o T_\parallel / B T_o\,]^{-1}$, the parallel pressure is given by $P_\parallel(\psi,B) = P(\psi)\,T_\perp(\psi,B) / T_\parallel(\psi)$, the perpendicular pressure is given by $P_\perp(\psi,B) = P(\psi)\,[T_\perp(\psi,B) / T_\parallel(\psi)]^2$, and the pressure anisotropy parameter is given by $\tau = 1 + (2P_\perp / B^2)\,[\,1 - P_\perp / P_\parallel\,]$, where $N(\psi)$ and $P(\psi) \approx N(\psi)T_\parallel(\psi)$ are the density and pressure in the isotropic limit, respectively.

4. Linearized Kinetic-MHD Eigenmode Equations

In terms of the perturbed quantities, the fluid displacement vector $\vec{\xi}$, the perturbed current density $\delta\vec{j}$, and the perturbed parallel and perpendicular pressures $\delta p_\parallel$ and $\delta p_\perp$, the linearized momentum equations can be obtained from Eqs.(2.19)-(2.21). The perturbed quantities are proportional to $\exp(-i\omega t)$, where ω is the frequency, and the fluid velocity $\vec{V} = -i\omega\vec{\xi}$. Since the parallel electric field $E_\parallel = 0$ from the Ohm's law, we have

$$\vec{B} \bullet \vec{A} + \vec{B} \bullet \nabla\Phi = 0, \tag{4.1}$$

where $\Phi = i\,\phi / \omega$. If we consider ϕ and $\vec{A}$ to be of the same order, then $\vec{E}_\perp = -\nabla_\perp \phi$ and $A_\perp$ contribution can be neglected because $(k_\perp c/\omega)^2 = (k_\perp V_A\, \omega_{pi} / \omega\, \omega_{ci})^2 >> 1$ for low frequency waves in typical space and laboratory plasma, where V_A is the Alfvén speed, ω_{pi} is the ion plasma frequency, and ω_{ci} is the ion cyclotron frequency. The linearized Ohm's law becomes

$$\vec{\xi} \times \vec{B} - \nabla_\perp \Phi = 0 . \tag{4.2}$$

Employing the Coulomb gauge $\nabla \cdot \vec{A} = 0$, the Ampere's law reduces to

$$\nabla^2 \vec{A} = -\delta\vec{j} . \tag{4.3}$$

We will consider low-frequency waves with perpendicular wavelength small compared to the parallel wavelength and to the equilibrium scale length. The perturbed transverse magnetic field is related to the electrostatic potential by $\delta\vec{B}_\perp = -\,i\,\nabla \times [\vec{B}(c\vec{B}\cdot\nabla\Phi/B^2)]$. With the perturbed pressures $\delta p_\parallel$ and $\delta p_\perp$ given by

$$\begin{pmatrix} \delta p_\parallel \\ \delta p_\perp \end{pmatrix} = \sum_j m_j \int d^3v\, \delta f_j \begin{pmatrix} 2(\varepsilon - \mu B) \\ \mu B \end{pmatrix} , \tag{4.4}$$

and from Eq.(2.19), the linearized parallel momentum equation describes the slow magnetosonic waves, which maintains the parallel pressure balance, and is given by

$$\rho\omega^2 \vec{B}\cdot\vec{\xi} - \vec{B}\cdot\nabla\delta p_\parallel - \frac{(P_\perp - P_\parallel)}{B^2}[\vec{B}\cdot\nabla(\vec{B}\cdot\delta\vec{B})] = 0 . \tag{4.5}$$

The linearized parallel current equation is obtained from Eq.(2.20) and Eqs.(4.1)-(4.3) and is given by

$$\vec{B}\cdot\nabla\left(\frac{\sigma\nabla_\perp^2}{B^2}\vec{B}\cdot\nabla\Phi\right) + \frac{\rho\omega^2}{B^2}\nabla_\perp^2\Phi - \frac{(\vec{B}\times\vec{\kappa})}{B^2}\cdot\nabla[\vec{B}\cdot\delta\vec{B} - \delta p_\parallel] = 0 , \tag{4.6}$$

which describes the transverse Alfvén waves (ballooning mode). From Eq.(2.21) the linearized perpendicular current equation becomes

$$\vec{B} \bullet \nabla[\frac{\sigma}{B^2} \vec{B} \bullet \nabla(\vec{B} \bullet \delta\vec{B})] + \frac{\rho\omega^2}{B^2} (\vec{B} \bullet \delta\vec{B}) + \nabla_\perp^2 [\vec{B} \bullet \delta\vec{B} + \delta p_\perp] \approx 0 , \qquad (4.7)$$

which describes the compressional Alfvén waves (drift mirror mode). The derivation of Eqs. (4.6) and (4.7) is given in Appendix B. Equation (4.5) basically describes the slow magnetosonic waves that maintain the pressure balance along the field line, and all the terms in Eq.(4.5) are smaller than terms in Eqs.(4.6) and (4.7) by $O(k_\parallel/k_\perp)$. Also note that Eq.(4.5) decouples from Eqs.(4.6) and (4.7). Thus, Eqs.(4.6) and (4.7) form the basis of the linear eigenmode equations for describing the coupling between the transverse and compressional Alfvén waves.

To obtain the perturbed pressure we shall proceed with the linearized gyrokinetic equation for all particle species. Since the parallel electric field vanishes, we obtain from Eq.(4.1) that

$$\phi - \frac{v_\parallel A_\parallel}{c} = [\frac{\partial}{\partial t} + \vec{v}_\parallel \bullet \nabla]\Phi . \qquad (4.8)$$

From Eq.(2.10), the perturbed particle distribution function δf can be written as

$$\delta f = -i\omega \frac{e}{m} \frac{\partial F}{\partial \varepsilon} \Phi (1 - J_o e^{iL_o}) + \frac{e}{mB} \frac{\partial F}{\partial \mu} (\frac{\partial}{\partial t} + \vec{v}_\parallel \bullet \nabla) \Phi (1 - J_o e^{iL_o})$$

$$- \frac{c}{B^2} \nabla F \bullet \vec{B} \times \nabla\Phi J_o e^{iL_o} - \frac{e}{mB} \frac{\partial F}{\partial \mu} \frac{v_\perp \delta B_\parallel}{c k_\perp} J_1 e^{iL_o} + \hat{g} e^{iL_o} , \qquad (4.9)$$

and the linearized gyrokinetic equation, Eq.(2.13), becomes

$$[\frac{\partial}{\partial t} + (\vec{v}_\parallel + \vec{v}_d) \bullet \nabla] \hat{g}$$

$$= [\frac{e}{m} \frac{\partial F}{\partial \varepsilon} \frac{\partial}{\partial t} - \frac{c\vec{B} \times \nabla F}{B^2} \bullet \nabla] [\vec{v}_d \bullet \nabla\Phi J_o - \frac{v_\perp \delta B_\parallel}{c k_\perp} J_1] . \qquad (4.10)$$

The total perturbed perturbed pressures are given by

$$\begin{pmatrix}\delta p_{\parallel}\\ \delta p_{\perp}\end{pmatrix} = -\frac{\vec{B}\times\nabla\Phi}{B^2}\bullet\tilde{\nabla}\begin{pmatrix}P_{\parallel}\\ P_{\perp}\end{pmatrix} + \frac{\vec{B}\bullet\delta\vec{B}}{B}\left(\frac{\partial}{\partial B}\right)_{\psi}\begin{pmatrix}P_{\parallel}\\ P_{\perp}\end{pmatrix} + \begin{pmatrix}\delta\hat{p}_{\parallel}\\ \delta\hat{p}_{\perp}\end{pmatrix}$$

$$+ \sum_j m\int d^3v\,\Big\{\Big[-\Big(\frac{e}{m}\frac{\partial F}{\partial\varepsilon}+\frac{e}{mB}\frac{\partial F}{\partial\mu}\Big)(i\omega\Phi)+\frac{c}{B^2}\nabla F\bullet\vec{B}\times\nabla\Phi\Big]\,[1-J_0^2]$$

$$-\frac{\mu}{B^2}\frac{\partial F}{\partial\mu}\vec{B}\bullet\delta\vec{B}\;\Big[1-\frac{\omega_c}{k_{\perp}v_{\perp}}J_0J_1\Big]\Big\}\begin{pmatrix}2(\varepsilon-\mu B)\\ \mu B\end{pmatrix}, \qquad (4.11)$$

where the summation is over the particle species j, and $\tilde{\nabla} = \nabla - \nabla B\,(\partial/\partial B)_{\psi}$. The nonadiabatic perturbed pressure, $\delta\hat{p}_{\parallel}$ and $\delta\hat{p}_{\perp}$, are given by

$$\begin{pmatrix}\delta\hat{p}_{\parallel}\\ \delta\hat{p}_{\perp}\end{pmatrix} = \sum_j m\int d^3v\;\hat{g}\exp(iL_o)\begin{pmatrix}2(\varepsilon-\mu B)\\ \mu B\end{pmatrix}, \qquad (4.12)$$

and contain the kinetic effects due to wave-particle resonances. The nonadiabatic particle distribution $\hat{g}$ can be integrated by writing Eq.(4.10) in the form.

$$\Big[\sigma_{\parallel}|v_{\parallel}|\frac{\partial}{\partial s} - i(\omega-\omega_d)\Big]\,\hat{g}_{\sigma_{\parallel}} = -iX, \qquad (4.13)$$

where

$$X = \Big[\frac{e}{m}\frac{\partial F}{\partial\varepsilon}\omega - i\frac{c\vec{B}\times\nabla F}{B^2}\bullet\nabla\Big]\,\Big[\vec{v}_d\bullet\nabla\Phi\,J_o - \frac{v_{\perp}\delta B_{\parallel}}{ck_{\perp}}J_1\Big], \qquad (4.14)$$

$\sigma_{\parallel} = \pm 1$ indicates the direction of the parallel velocity, s is the distance along the field line, and the magnetic drift frequency is $\omega_d = \vec{k}_{\perp}\bullet\vec{v}_d$. Assuming that particles are magnetically trapped within

the turning points, s_1 and s_2, Eq.(4.13) is a first order differential equation in s and can be integrated by neglecting finite banana width to give [Rutherford and Frieman, 1968; Taylor and Hastie, 1968; Chen and Hasegawa, 1991]

$$\hat{g}(\sigma_{\|}, s) = e^{i\sigma_{\|} I^{s}_{s_1}} \int_{s_1}^{s_2} \frac{ds'}{|v_{\|}|} X \left[\cos\left(I^{s'}_{s_1}\right) \cot\left(I^{s_2}_{s_1}\right) + \sin\left(I^{s'}_{s_1}\right)\right]$$

$$- i\sigma_{\|} \int_{s_1}^{s} \frac{ds'}{|v_{\|}|} X e^{i\sigma_{\|} I^{s}_{s'}}, \tag{4.15}$$

where $s_1 \le s \le s_2$, and

$$I^{s}_{s'} = \int_{s'}^{s} \frac{ds''}{|v_{\|}|} (\omega - \omega_d). \tag{4.16}$$

The detailed derivation of Eq.(4.15) is given in Appendix C.

Equations (4.6), (4.7), (4.11), (4.12), and (4.15) form a complete set of eigenmode equations for the eigenvalue ω and eigenfunctions Φ and $\vec{B} \cdot \delta\vec{B}$. It is quite complicated to integrate Eqs.(4.15) even computationally, and we need to further simplify these integral expressions analytically in order to reduce the computational efforts. The s' integration in Eq.(4.15) can be carried out by means of a Fourier series transformation rather than an integral representation. Computationally a more manageable series representation of Eqs.(4.15) is derived in Appendix C and is given by

$$\hat{g}(\sigma_{\|}, s) = e^{i\sigma_{\|}[\Gamma(\hat{\theta}+\pi)+W_d]} \sum_{p=-\infty}^{\infty} \{ \Psi^{p}_{-} \left[\cot\left(I^{s_2}_{s_1}\right) - i\right] e^{i\Gamma\pi} \frac{\sin(\Gamma+p)\pi}{(\Gamma+p)}$$

$$+ \Psi^{p}_{+} \left[\cot\left(I^{s_2}_{s_1}\right) + i\right] e^{-i\Gamma\pi} \frac{\sin(\Gamma-p)\pi}{(\Gamma-p)} \}$$

$$- \sigma_{\|} e^{i \sigma_{\|} [\Gamma \hat{\theta} + W_d]} \sum_{p=-\infty}^{\infty} \Psi^p_{\sigma\|} \{ e^{i (p - \sigma_{\|} \Gamma) \hat{\theta}} - e^{-i (p - \sigma_{\|} \Gamma) \pi} \} / (p - \sigma_{\|} \Gamma) , \tag{4.17}$$

where $\Gamma = (\omega - < \omega_d >) / 2\omega_b$, the bounce frequency is $\omega_b = \pi / [\int_{s_1}^{s_2} ds / | v_{\|} |]$, the bounce-averaged magnetic drift frequency is

$$< \omega_d > = (\omega_b / \pi) \int_{s_1}^{s_2} ds \, \omega_d / | v_{\|} | , \tag{4.18}$$

the angle-like particle trajectory variable is

$$\hat{\theta}(s) = 2\omega_b \int_{s_1}^{s} ds' / | v_{\|} | - \pi , \tag{4.19}$$

the deviation of the integrated magnetic drift frequency from its bounce-averaged value is

$$W_d(s) = - \int_{s_1}^{s} (ds' / | v_{\|} |) (\omega_d - < \omega_d >) , \tag{4.20}$$

the bounce-average of X for the p'th harmonic for particle parallel velocity direction $\sigma_{\|}$ is

$$\Psi^p_{\sigma\|} = (\omega_b / \pi) \int_{s_1}^{s_2} (ds \, X / | v_{\|} |) \, e^{-i [p \hat{\theta} + \sigma_{\|} W_d]} , \tag{4.21}$$

and note that with these definitions $\hat{\theta}(s_1) = - \pi$, $\hat{\theta}(s_2) = \pi$, and $W_d(s_1) = W_d(s_2) = 0$. The series representation has the clear advantage that it can be truncated if it converges quickly or if some particular resonance term is dominant. It also has the computational advantage that each term can be computed in advance of the iteration procedure for searching eigensolutions, and large savings in computational efforts can be realized.

It is clear from Eq.(4.17) that $(p \pm \Gamma) = 0$ does not give rise to resonances. Instead, the wave-particle resonance is contained in the $\cot\left(I_{s_1}^{s_2}\right)$ term. Noting that $I_{s_1}^{s_2} = \pi\,(\omega - <\omega_d>) / \omega_b$ and by using the Poisson sum formula [Morse and Feshbach, 1953] we have

$$\cot\left(I_{s_1}^{s_2}\right) = \sum_{\ell=-\infty}^{\infty} \frac{\omega_b}{\pi\,(\omega - <\omega_d> - \ell\omega_b)} \,. \tag{4.22}$$

The magnetic drift and bounce resonances are contained through the causality condition, i.e., $\omega = \omega + i\,0+$, so that

$$\frac{1}{(\omega - <\omega_d> - \ell\,\omega_b)} = \mathrm{Prin}\,\frac{1}{(\omega - <\omega_d> - \ell\,\omega_b)} + i\,\pi\,\delta(\omega - <\omega_d> - \ell\,\omega_b), \tag{4.23}$$

where Prin means the principal part.

It is instructive to calculate the resonance contribution to the nonadiabatic particle distribution which is obtained from Eqs.(4.15) and (4.23) and is given by

$$\mathrm{Res}[\hat{g}(\sigma_{\|}, s)] = e^{i\,\sigma_{\|} I_{s_1}^{s}} \int_{s_1}^{s_2} \frac{ds'}{|v_{\|}|} \times \cos\left(I_{s_1}^{s'}\right) \sum_{\ell=-\infty}^{\infty} i\,\omega_b\,\delta(\omega - <\omega_d> - \ell\,\omega_b), \tag{4.24}$$

Since

$$I_{s_1}^{s'} = \Gamma\,[\hat{\theta}(s') + \pi] + W_d(s'), \tag{4.25}$$

and $\Gamma = \ell / 2$, Eq.(4.24) can be carried out and reduces to

$$\mathrm{Res}[\hat{g}(\sigma_{\|}, s)] = \sum_{\ell=-\infty}^{\infty} i\,\omega_b\,\delta(\omega - <\omega_d> - \ell\,\omega_b)\; e^{i\,\sigma_{\|}\,[\ell\,(\hat{\theta} + \pi)\,/\,2 + W_d]}$$

$$\int_{s_1}^{s_2} \frac{ds'}{|v_{\parallel}|} X(s') \{\cos[\ell\,\hat{\theta}(s')/2 + W_d(s')]\cos(\ell\pi/2) - \sin[\ell\,\hat{\theta}(s')/2 + W_d(s')]\sin(\ell\pi/2)\}, \qquad (4.26)$$

If the equilibrium magnetic field has a north-south symmetry with respect to the equator, both $\hat{\theta}(s')$ and $W_d(s')$ are antisymmetric with respect to the equator. Thus in Eq.(4.26) the trapped particle orbit integration vanishes for even integer ℓ if X is antisymmetric with respect to the equator. Hence, for perturbations with Φ and $\vec{B}\bullet\delta\vec{B}$ having antisymmetric structures along the north-south symmetric equilibrium magnetic field lines, the magnetic drift-bounce resonance contribution to the nonadiabatic particle distribution results from odd ℓ. Similarly, the trapped particle orbit integration in Eq.(4.26) vanishes for odd integer ℓ if X is symmetric with respect to the equator, and for perturbations with Φ and $\vec{B}\bullet\delta\vec{B}$ having symmetric structures along the north-south symmetric equilibrium magnetic field lines, the magnetic drift-bounce resonance contribution to the nonadiabatic particle distribution survives only for even ℓ. We note that these conclusions derived from Eqn. (4.26) were previously obtained for a more complicated magnetic field in the toroidal system [Cheng, 1989].

Physically the $(\omega - \langle\omega_d\rangle) - \ell\omega_b = 0$ ($\ell \neq 0$) magnetic drift-bounce resonance behavior can be best illustrated by taking $\omega = 0$ so that the wave is static in time. As the particles precess in the toroidal ϕ direction in a π toroidal phase of the wave, they also excute ($|\ell|/2$) complete bounce motions along the field line between the turning points s_1 and s_2 for a time $t = \pi/\omega_b$. For simplicity, we assume that during the time $t = \pi/\omega_b$ the toroidal phase contribution to the wave changes from being positive in the first $\pi/2$ phase to being negative in the second $\pi/2$ phase. For a symmetry structures of Φ and $\vec{B}\bullet\delta\vec{B}$ along the north-south symmetric equilibrium magnetic field lines, the sign of the wave amplitude can be pictured in the (s,ϕ) space [Southwood and Kivelson, 1982]. If Φ and $\vec{B}\bullet\delta\vec{B}$ have antisymmetric structures along the north-south symmetric equilibrium magnetic field lines, the even ℓ resonances average out due to complete bounce motions of the particle. On the other hand, the odd ℓ resonances will survive due to incomplete particle bounce motions. The $|\ell| = 1$ resonance contribution will be largest since the particle experiences same sign wave amplitude during the time $\tau = \pi/\omega_b$. But the higher odd $|\ell|$ resonance contribution will have smaller contribution. This is because during the time $t = \pi/\omega_b$ the particle experiences one sign wave amplitude for part of the time and sees the opposite sign wave amplitude for other part of the

time. The above conclusion can be generalized to situations with arbitrary toroidal phase contribution of the wave during the time $t = \pi / \omega_b$ with the exception that those particles whose beginning and end turning points coincide with points of zero wave amplitude will experience no resonance contribution. Physical picture can be similarly drawn for perturbations with Φ and $\vec{B}\bullet\delta\vec{B}$ having symmetric structures along the north-south symmetric equilibrium magnetic field lines. In general the wave frequency $\omega \neq 0$, but similar physical picture can be obtained in the wave moving frame.

5. Guiding Center Drift Kinetic Approximation

To make further analytical progress and gain a better physical insight on the stability properties, we shall simplify the dynamics by taking the guiding center drift kinetic approximation with $(k_\perp v_\perp/\omega_c) << 1$ (the particle gyroradius is very small compared to the perpendicular wavelength) for all particle species. The perturbed particle distribution is then given by

$$\delta f = - \frac{c}{B^2} \nabla F \bullet \vec{B} \times \nabla \Phi - \frac{\mu}{B^2} \frac{\partial F}{\partial \mu} \vec{B} \bullet \delta \vec{B} + \hat{g} , \tag{5.1}$$

where the drift kinetic equation for $\hat{g}$ is given by Eq.(4.13), but with X given by

$$X = [\frac{e}{m} \frac{\partial F}{\partial \varepsilon} \omega - i \frac{c \vec{B} \times \nabla F}{B^2} \bullet \nabla] [\vec{v}_d \bullet \nabla \Phi - \frac{i\omega \mu \delta B_\parallel}{e}] , \tag{5.2}$$

The perturbed pressures are obtained from Eq.(4.11) and are given by

$$\begin{pmatrix} \delta p_\parallel \\ \delta p_\perp \end{pmatrix} = - \frac{\vec{B} \times \nabla \Phi}{B^2} \bullet \tilde{\nabla} \begin{pmatrix} P_\parallel \\ P_\perp \end{pmatrix} + \frac{\vec{B} \bullet \delta \vec{B}}{B} \left(\frac{\partial}{\partial B} \right)_\psi \begin{pmatrix} P_\parallel \\ P_\perp \end{pmatrix} + \begin{pmatrix} \delta \hat{p}_\parallel \\ \delta \hat{p}_\perp \end{pmatrix} , \tag{5.3}$$

where $\tilde{\nabla} = \nabla - \nabla B \, (\partial/\partial B)_\psi$. The linearized parallel current equation, Eq.(4.6), becomes

$$\vec{B} \bullet \nabla (\frac{\sigma \nabla_\perp^2}{B^2} \vec{B} \bullet \nabla \Phi) + \frac{\rho \omega^2}{B^2} \nabla_\perp^2 \Phi + \frac{(\vec{B} \times \vec{\kappa})}{B^2} \bullet \nabla [\frac{\vec{B} \times \tilde{\nabla} P_\parallel}{B^2} \bullet \nabla \Phi + \delta \hat{p}_\parallel]$$

$$+ \frac{[\vec{B}\times\nabla(B^2/2)]}{B^4}\cdot\nabla\left[\frac{\vec{B}\times\tilde{\nabla P}_\perp}{B^2}\cdot\nabla\Phi+\delta\hat{p}_\perp\right]-\frac{\vec{B}\times\tilde{\nabla P}_\perp}{B^4}\cdot\nabla(\vec{B}\cdot\delta\vec{B})=0\,, \quad (5.4)$$

and the linearized perpendicular current equation, Eq.(4.7), becomes

$$\vec{B}\cdot\nabla\left[\frac{\sigma}{B^2}\,\vec{B}\cdot\nabla(\vec{B}\cdot\delta\vec{B})\right]+\frac{\rho\omega^2}{B^2}(\vec{B}\cdot\delta\vec{B})$$

$$+\nabla_\perp^2\left[\tau\vec{B}\cdot\delta\vec{B}+\frac{\vec{B}\times\tilde{\nabla P}_\perp}{B^2}\cdot\nabla\Phi+\delta\hat{p}_\perp\right]=0\,, \quad (5.5)$$

Equations (5.4)-(5.5) are identical to Eq.(1a) and (1b) previously presented in the paper by Cheng and Lin [1987] but without the hot particle finite Larmor radius correction, $(\omega_{*\perp}/\omega)$ term, in Eq.(1a). Eqs. (1a) and (1b) in the paper by Cheng and Lin [1987] are derived from the general frequency gyrokinetic equation for all particle species. Thus we have demonstrated that the kinetic-MHD model indeed contains the essential physics for low frequency phenomena. They form the integro-differential eigenmode equations for the low-frequency transverse and compressional Alfvén waves with the perpendicular wavelength much shorter than the parallel wavelength. The kinetic effect due to trapped particles is included in the $\delta\hat{p}_\perp$ and $\delta\hat{p}_\parallel$ terms. The coupling between the compressional and transverse perturbed magnetic field is due to finite perpendicular pressure gradient, $\tilde{\nabla P}_\perp \neq 0$, and the perturbed trapped particle pressures $\delta\hat{p}_\perp$ and $\delta\hat{p}_\parallel$. From Eq.(5.4) we see that the transverse shear Alfvén wave in a $\beta = O(1)$ plasma can be strongly destabilized by the curvature and gradient-B terms to excite ballooning modes. Eq.(5.5) indicates that the compressional Alfvén waves can be destabilized by the pressure anisotropy to excite mirror type modes. The eigenmode structure of the drift mirror instability was obtained by analyzing these two equations both analytically and numerically and by including trapped particle effects [Cheng and Lin, 1987; Takahashi et al., 1990] to explain successfully the multi-satellite observation of the antisymmetric field-aligned structure of the compressional magnetic field of Pc 5 waves [Takahashi et al., 1987]. In general, to obtain quantitative eigensolutions of the coupled eigenmode equations, extensive numerical works are required.

6. Quadratic Form, Energy Principle, and Stability Property

A quadratic form can be derived from Eqs. (5.4) and (5.5) and provides significant insights to the stability properties. By adopting the WKB ansatz, Eq.(2.9) and assuming that the perturbed quantities vanish at the end points of the field line, we obtain the quadratic form

$$D(\omega) = \delta K - \delta W_f - \delta W_k = 0 , \tag{6.1}$$

where the inertia energy is given by

$$\delta K = \omega^2 \int \frac{ds}{B} \frac{\rho}{B^2} \left[k_\perp^2 |\tilde{\Phi}|^2 + \frac{|\vec{B} \cdot \delta\vec{B}|^2}{k_\perp^2 B^2} \right] \tag{6.2}$$

with $\tilde{\Phi} = -i\,\Phi = \phi / \omega$, the fluid potential energy is given by

$$\delta W_f = \int \frac{ds}{B} \left\{ \frac{\sigma}{B^2} k_\perp^2 |\vec{B} \cdot \nabla\tilde{\Phi}|^2 + \frac{\sigma}{B^2 k_\perp^2} |\vec{B} \cdot \nabla(\vec{B} \cdot \delta\vec{B})|^2 \right.$$

$$\left. + \tau \left| \frac{\vec{B} \cdot \delta\vec{B}}{B} - \frac{\vec{B} \times \vec{k}_\perp}{\tau B^3} \cdot \tilde{\nabla} P_\perp \tilde{\Phi} \right|^2 - \alpha_p |k_\perp \tilde{\Phi}|^2 \right\} \tag{6.3}$$

with

$$\alpha_p = \left(\frac{\vec{B} \times \vec{k}_\perp \cdot \vec{\kappa}}{k_\perp B} \right) \left[\left(\frac{\sigma}{\tau} \right) \frac{\vec{B} \times \vec{k}_\perp}{k_\perp B^3} \cdot \tilde{\nabla} P_\perp + \frac{\vec{B} \times \vec{k}_\perp}{k_\perp B^3} \cdot \tilde{\nabla} P_\parallel \right] , \tag{6.4}$$

and the kinetic potential energy due to all species is

$$\delta W_k = \int \frac{ds}{B} \left\{ \left[\frac{\vec{B} \cdot \delta\vec{B}}{B^2} - \frac{\vec{B} \times \vec{k}_\perp \cdot \nabla(B^2/2)}{B^4} \tilde{\Phi} \right]^* \delta\hat{p}_\perp - \frac{\vec{B} \times \vec{k}_\perp \cdot \vec{\kappa}}{B^2} \tilde{\Phi}^* \delta\hat{p}_\parallel \right\} . \tag{6.5}$$

Eq. (6.3) clearly displays the various fluid free energy sources. In particular, if $\sigma > 0$ (i.e. $1 + (P_\perp - P_\parallel) / B^2 > 0$) and $\tau > 0$ (i.e. $1 + (1/B)(\partial P_\perp / \partial B)_\psi > 0$) are satisfied everywhere in the plasma, the magnetosphere is stable to the well-known MHD "firehose" and "mirror" instabilities, respectively

[Grad, 1967]. The third term drives pressure gradient ballooning modes in the bad curvature region where $\alpha_p > 0$.

The quadratic form, Eq.(6.1), is not Hermitian, and there is no energy principle. However if δW_k is small compared with δW_f and can be neglected, then Eq.(6.1) is an energy principle and the variational technique can be applied to obtain eigenvalue and eigenfunction. In the magnetospheric ring current region, it was shown by Cheng and Lin [1987] that perturbations with $\tilde{\Phi}$ and $\vec{B}\cdot\delta\vec{B}$ having antisymmetric structures along the north-south symmetric equilibrium magnetic field lines are most unstable, and in the limit $(\omega - \omega_d) << \omega_b$, $\delta\hat{p}_{\parallel}$ and $\delta\hat{p}_{\perp}$ are of the order of (ω/ω_b) smaller since the contributions from the magnetic drift resonance vanishes. Therefore, two parameters, α_p and τ, will determine the stability of the ballooning modes and the drift mirror modes in the ring current plasma. In the limit that the transverse and the compressional perturbed magnetic field decouple, the ballooning/interchange instability can occur if $\alpha_p > 0$ with perturbation localized around the region where $\alpha_p > 0$, and if $\tau < 0$, drift mirror mode can be unstable with perturbation localized around the region where $\tau < 0$. In general, the transverse and the compressional perturbed magnetic field couple, and the stability properties will be modified. It was shown [Cheng, Lin, 1988] that the threshold for destabilizing the drift mirror modes is reduced due to this coupling.

When the wave particle resonance is important, the $(\omega - <\omega_d>) = \pm \ell\omega_b$ magnetic drift-bounce resonance contribution from δW_k must be considered. The stability of a marginally stable MHD wave (with growth rate smaller than real frequency) due to wave-particle resonances can be obtained perturbatively from the quadratic form, Eq. (6.1). We write the mode frequency as $\omega = \omega_r + i\gamma$ and assume that the growth rate is small ($|\gamma| << |\omega_r|$). Then the frequency of the MHD wave is given by

$$\omega_r^2 \approx \{\delta W_f + \mathrm{Prin}[\delta W_k]\}/\delta K , \tag{6.6}$$

and the growth rate due to wave-particle resonances is given by

$$\gamma \approx \mathrm{Res}[\delta W_k] / 2i\omega_r \delta K , \tag{6.7}$$

where $\mathrm{Prin}[\delta W_k]$ and $\mathrm{Res}[\delta W_k]$ are the principal part and resonance contribution, respectively. The wave particle resonances due to all particle species are retained in $\mathrm{Res}[\delta W_k]$. If the $\mathrm{Prin}[\delta W_k]$ contribution can be neglected in Eq.(6.6), the lowest order eigenvalue ω_r and corresponding

eigenfunction are determined from the solutions of the appropriate eigenmode equations, Eqs. (5.4) and (5.5).

To resolve the nature of the magnetic pulsations observed by space craft, it is important to determine these stability conditions from the particle distributions obtained from satellite measurements. A correlation study between these instability parameters obtained from AMPTE/CCE particle data and the occurrence of Pc wave events is currently being pursued [Cheng et al., 1990].

7. Summary and Conclusion

In the paper we have presented a hybrid kinetic-MHD model for describing low-frequency phenomena in plasmas that consist of two components of plasmas: the core component has low energy and satisfies MHD description, the energetic component has low density and MHD description is not valid for its dynamics. The hybrid kinetic-MHD model treats the low energy core component by MHD description, the energetic component by kinetic approach such as the gyrokinetic equation or Vlasov equation, and the coupling between the dynamics of these two components through plasma pressure in the momentum equation. The momentum equation is decomposed into three scalar equations that determine the dynamics of slow magnetosonic wave, transverse Alfvén wave, and fast magnetosonic (compressional Alfvén) waves, respectively, in the presence of energetic particles. The kinetic-MHD model optimizes both the physics contents and the theoretical efforts in studying low frequency phenomena. The kinetic-MHD model presented here also properly takes into account the dynamics of high-β ($\beta \sim O(1)$) plasma with pressure anisotropy in general magnetic field geometries and is useful in studying low frequency MHD type instabilities, wave propagation, and plasma transport processes. It should be noted that the applicability of the kinetic-MHD model presented here is not limited to the magnetospheric and toroidal plasmas; it is applicable to any plasma system where parallel electric field effect is negligibly small. The kinetic-MHD model can also be easily modified to include the core plasma kinetic effects if necessary.

To demonstrate the validity of the kinetic-MHD model, two coupled eigenmode equations are derived to describe the coupling between the transverse Alfvén type and compressional Alfvén type waves in the linearized limit. The eigenmode equations are identical to those derived from the full gyrokinetic equation in the low frequency limit [Berk et al., 1983; Cheng and Lin, 1987]. The transverse Alfvén wave equation shows that the shear Alfvén type wave can be strongly destabilized

by the combined effect of the magnetic field curvature and the plasma pressure gradient to excite ballooning mode. The compressional Alfvén wave equation indicates that the drift mirror mode can be destabilized by the pressure anisotropy. By analyzing the coupled eigenmode equations both analytically and numerically, the eigenmode structure of the drift mirror instability was obtained [Cheng and Lin, 1987; Takahashi et al., 1990] to explain successfully the multi-satellite observation of antisymmetric field-aligned structure of the compressional magnetic field of Pc 5 waves [Takahashi et al., 1987] in the magnetospheric ring current plasma. The coupling between the compressional and transverse magnetic field is due to finite perpendicular pressure gradient and the trapped particle perturbed pressures.

The solution of the linearized gyrokinetic equation for trapped particles is also presented in terms of both an integral form and a series representation. It was found that if the magnetospheric equilibrium magnetic field has a north-south symmetry with respect to the equator, the $(\omega - \langle\omega_d\rangle) = \pm \ell\omega_b$ magnetic drift-bounce resonance contribution to the nonadiabatic particle distribution is due to odd ℓ for perturbations with Φ and $\vec{B}\bullet\delta\vec{B}$ having antisymmetric structures with respect to the equatorial plane along the north-south symmetric equilibrium magnetic field lines. Similarly, if Φ and $\vec{B}\bullet\delta\vec{B}$ have symmetric structures along the north-south symmetric equilibrium magnetic field lines, the $(\omega - \langle\omega_d\rangle) = \pm \ell\omega_b$ magnetic drift-bounce resonance contribution to the nonadiabatic particle distribution is due to even ℓ.

A quadratic form is derived to demonstrate the stability of the low-frequency transverse and compressional Alfvén wave type instabilities in terms of the pressure anisotropy parameter τ and the magnetic field curvature-pressure gradient parameter α_p as defined in Eqs.(3.7) and (6.4), respectively. A procedure for determining the stability of a marginally stable MHD type waves due to wave-particle resonances is also presented. To resolve the nature of the magnetic pulsations observed by space crafts in the magnetosphere, it is important to determine these stability conditions from the particle distributions obtained from satellite measurements. A correlation study between these instability parameters obtained from AMPTE/CCE particle data and the occurrence of Pc wave events is currently being pursued [Cheng et al., 1990].

Appendix A: Derivation of the Scalar Momentum Equations, Eqs.(2.19)-(2.21)

The three scalar momentum equations can be obtained from Eq.(2.17) by first operating on Eq.(2.17) with $(\vec{b}\bullet)$. By noting that

$$b^2 \vec{b} \bullet \nabla \sigma = \vec{b} \bullet \nabla (P_\perp - P_\parallel) - [(P_\perp - P_\parallel) / b^2] \vec{b} \bullet \nabla b^2, \tag{A.1}$$

and

$$\vec{b} \bullet [\vec{b} \bullet \nabla \vec{b}] = \vec{b} \bullet \nabla (b^2 / 2), \tag{A.2}$$

the parallel momentum balance equation, Eq.(2.19), is easily obtained.

To obtain Eq.(2.20), we operate on Eq.(2.17) with $\vec{b} \bullet \nabla \times$ and make use of the following equalities:

$$\vec{b} \bullet \nabla \times (\rho \frac{d}{dt} \vec{V}) = \nabla \bullet (\rho \frac{d}{dt} \vec{V} \times \vec{b}) + \rho \frac{d}{dt} \vec{V} \bullet \vec{j}, \tag{A.3}$$

$$\vec{b} \bullet \nabla \times (\sigma \vec{j} \times \vec{b}) = \vec{b} \bullet \nabla (\sigma \vec{j} \bullet \vec{b}) + \vec{j} \bullet \nabla (\sigma b^2), \tag{A.4}$$

$$\vec{b} \bullet \nabla \times [(\sigma - 1) \nabla (b^2/2)] = \vec{b} \times \nabla \sigma \bullet \nabla (b^2/2), \tag{A.5}$$

and

$$\vec{b} \bullet \nabla \times (\vec{b} \ \vec{b} \bullet \nabla \sigma) = \vec{b} \bullet \vec{j} \ \vec{b} \bullet \nabla \sigma. \tag{A.6}$$

By adding Eqs.(A.3)-(A.6) we can express the parallel current equation in the following form:

$$\nabla \bullet (\rho \frac{d}{dt} \vec{V} \times \vec{b}) + \rho \frac{d}{dt} \vec{V} \bullet \vec{j}$$

$$= \vec{b} \bullet \nabla (\sigma \vec{j} \bullet \vec{b}) + \vec{j} \bullet \nabla (\sigma b^2) + \vec{b} \times \nabla \sigma \bullet \nabla (b^2/2) + \vec{b} \bullet \vec{j} \ \vec{b} \bullet \nabla \sigma$$

$$= b^2 \vec{b} \bullet \nabla (\sigma \vec{j} \bullet \vec{b} / b^2) - [\vec{b} \times \nabla (b^2/2) / b^2 + \vec{j}_\perp] \bullet \nabla (\sigma b^2). \tag{A.7}$$

From Eq.(2.17) and recalling the identities

$$\vec{j} \times \vec{b} + \nabla (b^2/2) = \vec{b} \bullet \nabla \vec{b}, \tag{A.8}$$

and

$$\vec{b} \times \nabla (b^2/2) / b^2 + \vec{j}_\perp = \vec{b} \times [(\frac{\vec{b}}{b}) \bullet \nabla (\frac{\vec{b}}{b})], \tag{A.9}$$

we have

$$[\vec{b}\times\nabla(b^2/2)/b^2+\vec{j}_\perp]\bullet\nabla(\sigma b^2)$$
$$=\vec{b}\times[(\frac{\vec{b}}{b})\bullet\nabla(\frac{\vec{b}}{b})]\bullet\nabla(b^2/2-P_\parallel)-\rho\frac{d}{dt}\vec{V}\bullet[\vec{b}\times\nabla(b^2/2)/b^2+\vec{j}_\perp]. \qquad (A.10)$$

Substituting Eq.(A.10) into Eq.(A.7), the parallel current equation, Eq.(2.20), is obtained.

To obtain Eq.(2.21) we first operate Eq.(17) with $\vec{b}\times$ operator, and we have

$$\vec{b}\times\rho\frac{d}{dt}\vec{V}=\sigma b^2\vec{j}_\perp-\vec{b}\times\nabla(P_\perp+b^2/2)+\sigma\vec{b}\times\nabla(b^2/2). \qquad (A.11)$$

Operating on Eq.(A.11) with the operator $\vec{b}\bullet\nabla\times$, and the following relations are found:

$$\vec{b}\bullet\nabla\times(\sigma b^2\vec{j}_\perp)=-\sigma b^2\vec{b}\bullet\nabla^2\vec{b}+\vec{j}\times\vec{b}\bullet\nabla(\sigma b^2)-\sigma(\vec{j}\bullet\vec{b})^2, \qquad (A.12)$$

$$\vec{b}\bullet\nabla\times[\vec{b}\times\nabla(P_\perp+b^2/2)]$$
$$=b^2\nabla^2(P_\perp+b^2/2)+(\nabla b^2+\vec{j}\times\vec{b})\bullet\nabla(P_\perp+b^2/2)-\vec{b}\bullet\nabla[\vec{b}\bullet\nabla(P_\perp+b^2/2)], \qquad (A.13)$$

and

$$\vec{b}\bullet\nabla\times[\vec{b}\times\nabla(P_\perp+b^2/2)]=\nabla(b^2/2)\bullet\nabla(\sigma b^2)+\sigma b^2\nabla^2(b^2/2)$$
$$-\vec{b}\bullet\nabla[\sigma\vec{b}\bullet\nabla(b^2/2)]+\sigma(\vec{j}\times\vec{b})\bullet\nabla(b^2/2). \qquad (A.14)$$

The perpendicular current equation, Eq.(2.21), is then obtained from Eqs.(A.11)-(A.14).

Appendix B: Derivation of the Linearized Eigenmode Equations, Eqs.(4.6)-(4.7)

Consider low-frequency waves with perpendicular wavelength small compared to the parallel wavelength and to the equilibrium scale length, i.e., $|\nabla_\perp\Phi| >> |\nabla_\parallel\Phi|$. In Eq.(2.20) the first three terms are dominant terms. From Eq.(4.1) the parallel component of the Ampere's law, Eq.(4.3), approximately reduces to

$$\vec{B}\bullet\delta\vec{j}=-\nabla^2(\vec{B}\bullet\vec{A})\approx\nabla_\perp^2\vec{B}\bullet\nabla\Phi. \qquad (B.1)$$

Also from Eq.(4.2) the first term in Eq.(2.20) reduces to

$$\nabla \cdot (\rho \vec{B} \times \partial \vec{V}/\partial t) = \nabla \cdot (\rho \omega^2 \vec{\xi} \times \vec{B}) = \rho \omega^2 \nabla_\perp{}^2 \Phi. \qquad (B.2)$$

Then, the linearized parallel current equation reduces to Eq.(4.6) by ignoring terms which are smaller by $O(k_\parallel/k_\perp)$.

Employing the Ohm's law and the Faraday's law the linearized inertia term in Eq.(2.21) becomes

$$\vec{B} \cdot \nabla \times (\rho \vec{B} \times \partial \vec{V}/\partial t) = \vec{B} \cdot \nabla \times (-i\rho\omega \vec{E}) = \rho \omega^2 \vec{B} \cdot \delta \vec{B}. \qquad (B.3)$$

The second and third terms in Eq.(2.21) can be combined to give $B^2 \nabla_\perp^2 [\vec{B} \cdot \delta \vec{B} + \delta p_\perp]$, and the fourth term represents parallel wave propagation and is kept to avoid singularity associated with the zero of $\nabla_\perp^2 [\vec{B} \cdot \delta \vec{B} + \delta p_\perp]$. The other terms are smaller by at least $O(k_\parallel/k_\perp)$ and can be neglected. The linearized perpendicular current equation, Eq.(4.7), is obtained by keeping these first four terms in Eq.(2.21).

Appendix C: Solution of the Gyrokinetic Equation

Assuming that particles are magnetically trapped along the field line within the turning points, s_1 and s_2, Eq.(4.13) is a first order differential equation in s and can be integrated to give the nonadiabatic particle distribution

$$\hat{g}(\sigma_\parallel, s) = \hat{g}(\sigma_\parallel, s_3)\, e^{i\sigma_\parallel I_{s_3}^{s}} - i\sigma_\parallel \int_{s_3}^{s} \frac{ds'}{|v_\parallel|} X\, e^{i\sigma_\parallel I_{s'}^{s}}, \qquad (C.1)$$

where $s_1 \le s_3 \le s_2$, and $I_{s'}^{s}$ is defined by Eq.(4.16). Note that to arrive at Eq.(C.1), we have assumed that typical particle radial excursions away from the flux surface (eg. trapped particle

banana width) along the unperturbed trajectory are assumed to be small compared to the equilibrium scale length. From Eq.(C.1) we have

$$\hat{g}(+1, s_2) = \hat{g}(+1, s_1)\, e^{i I_{s_1}^{s_2}} - i \int_{s_1}^{s_2} \frac{ds'}{|v_{\|}|} X\, e^{-i I_{s_2}^{s'}}, \tag{C.2}$$

and

$$\hat{g}(-1, s_1) = \hat{g}(-i, s_2)\, e^{i I_{s_1}^{s_2}} + i \int_{s_1}^{s_2} \frac{ds'}{|v_{\|}|} X\, e^{i I_{s_1}^{s'}}, \tag{C.3}$$

With the boundary conditions at the turning points, $\hat{g}(+1, s_1) = \hat{g}(-1, s_1)$ and $\hat{g}(+1, s_2) = \hat{g}(-1, s_2)$, we substitute Eq.(C.2) into Eq.(C.3) to eliminate $\hat{g}(\sigma_{\|}, s_2)$ and obtain after some simple algebra

$$\hat{g}(\sigma_{\|}, s_1) = \int_{s_1}^{s_2} \frac{ds'}{|v_{\|}|} X \left[\cos(I_{s_1}^{s'}) \cot(I_{s_1}^{s_2}) + \sin(I_{s_1}^{s'})\right]. \tag{C.4}$$

By choosing s_3 to be s_1 in Eq.(C.1) and making use of Eq.(C.4) we obtain the solution of the gyrokinetic equation, Eq.(4.15),

$$\hat{g}(\sigma_{\|}, s) = e^{i \sigma_{\|} I_{s_1}^{s}} \int_{s_1}^{s_2} \frac{ds'}{|v_{\|}|} X \left[\cos(I_{s_1}^{s'}) \cot(I_{s_1}^{s_2}) + \sin(I_{s_1}^{s'})\right]$$

$$- i \sigma_{\|} \int_{s_1}^{s} \frac{ds'}{|v_{\|}|} X\, e^{i \sigma_{\|} I_{s'}^{s}}, \tag{C.5}$$

The following useful forms are easily derived from Eq.(C.5):

$$\frac{1}{2}\sum_{\sigma_{\|}} \hat{g}(\sigma_{\|}, s) = \cos\left(I^{s}_{s_1}\right) \int_{s_1}^{s_2} \frac{ds'}{|v_{\|}|} X \left[\cos\left(I^{s'}_{s_1}\right) \cot\left(I^{s_2}_{s_1}\right) + \sin\left(I^{s'}_{s_1}\right)\right]$$

$$- \int_{s_1}^{s} \frac{ds'}{|v_{\|}|} X \sin\left(I^{s}_{s'}\right), \qquad \text{(C.6)}$$

and

$$\frac{1}{2}\sum_{\sigma_{\|}} \sigma_{\|}\, \hat{g}(\sigma_{\|}, s) = i \sin\left(I^{s}_{s_1}\right) \int_{s_1}^{s_2} \frac{ds'}{|v_{\|}|} X \left[\cos\left(I^{s'}_{s_1}\right) \cot\left(I^{s_2}_{s_1}\right) + \sin\left(I^{s'}_{s_1}\right)\right]$$

$$- i \int_{s_1}^{s} \frac{ds'}{|v_{\|}|} X \cos\left(I^{s}_{s'}\right). \qquad \text{(C.7)}$$

It is quite complicated to integrate Eqs.(C.5) - (C.7) even computationally, and we need to further simplify these integral expressions analytically in order to reduce the computational efforts. The s' integration in Eq.(C.7) can be carried out by means of a Fourier series transform in the angle-like variable, $\hat{\theta}(s)$, defined by Eq.(4.19). Specifically, the Fourier transform is taken as

$$X\, e^{-i\sigma_{\|} W_d} = \sum_{p=-\infty}^{\infty} \Psi^{p}_{\sigma\|}\, e^{ip\hat{\theta}}, \qquad \text{(C.8)}$$

with the inverse Fourier transformation

$$\Psi^{p}_{\sigma\|} = \frac{1}{2\pi} \int_{-\pi}^{\pi} d\hat{\theta}\, X\, e^{-i\left[p\hat{\theta} + \sigma_{\|} W_d\right]}, \qquad \text{(C.9)}$$

where we have made use of the definitions, Eqs(4.18)-(4.20). With $\Gamma = (\omega - < \omega_d >) / 2\omega_b$, the bounce frequency $\omega_b = \pi / [\int_{s_1}^{s_2} ds / | v_\parallel |]$, and writing $\hat{\theta}(s) = \hat{\theta}$, and $\hat{\theta}(s') = \hat{\theta}'$, then

$$I_{s'}^{s} = \Gamma [\hat{\theta} - \hat{\theta}'] + W_d(s) - W_d(s') . \tag{C.10}$$

Since $\hat{\theta}(s_1) = -\pi$, $\hat{\theta}(s_2) = \pi$, and $W_d(s_1) = W_d(s_2) = 0$, we have

$$p\hat{\theta}' - W_d(s') + I_{s_1}^{s'} = (p + \Gamma) \hat{\theta}' + \Gamma \pi , \tag{C.11}$$

$$p\hat{\theta}' + W_d(s') - I_{s_1}^{s'} = (p - \Gamma) \hat{\theta}' - \Gamma \pi , \tag{C.12}$$

$$p\hat{\theta}' + \sigma_\parallel W_d(s') + \sigma_\parallel I_{s'}^{s} = (p - \sigma_\parallel \Gamma) \hat{\theta}' + \sigma_\parallel \Gamma \hat{\theta} + \sigma_\parallel W_d(s) , \tag{C.13}$$

and Eq.(C.7) becomes

$$\hat{g}(\sigma_\parallel, s) = e^{i \sigma_\parallel I_{s_1}^{s}} \int_{-\pi}^{\pi} \frac{d\hat{\theta}'}{4\omega_b} \sum_{p=-\infty}^{\infty} [\Psi_-^p [\cot (I_{s_1}^{s_2}) - i] e^{i [(p + \Gamma) \hat{\theta}' + \Gamma \pi]}$$

$$+ \Psi_+^p [\cot (I_{s_1}^{s_2}) + i] e^{i [(p - \Gamma) \hat{\theta}' - \Gamma \pi]}]$$

$$- i \sigma_\parallel \int_{-\pi}^{\hat{\theta}} \frac{d\hat{\theta}'}{2\omega_b} \sum_{p=-\infty}^{\infty} \Psi_{\sigma\parallel}^p e^{i [(p - \sigma_\parallel \Gamma) \hat{\theta}' + \sigma_\parallel \Gamma \hat{\theta} + \sigma_\parallel W_d(s)]} \tag{C.14}$$

Integrating over $\hat{\theta}'$ in Eq.(C.14) we obtain the Fourier series representation of the nonadiabatic particle distribution given by Eq.(4.17).

ACKNOWLEDGMENTS

The author would like to thank Dr. M. G. Kivelson for useful discussion. This work was supported by NSF Grant No. ATM-8911638 and DoE Contract No. DE-AC02-76-CHO-3073.

REFERENCES

Berk, H. L., C. Z. Cheng, M. N. Rosenbluth, and J. W. Van Dam, Finite Larmor radius stability theory of ELMO Bumpy Torus plasmas, Phys. Fluids 26, 2642, 1983.

Brizard, A., Nonlinear gyrokinetic Maxwell-Vlasov equations using magnetic co-ordinates, J. Plasma Phys. 41, 541, 1989.

Chen, L., R. B. White, and M. N. Rosenbluth, Excitation of internal kink modes by trapped energetic beam ions, Phys. Rev. Lett. 52, 1122, 1984.

Chen, L., and A. Hasegawa, Kinetic theory of geomagnetic pulsations 1. Internal excitations by energetic particles, J. Geophys. Res. 96, 1503, 1991.

Cheng, C. Z., The integration of Vlasov equation for a magnetized plasma, J. Comput. Phys. 24, 348, 1977.

Cheng, C. Z., and H. Okuda, New three-dimensional simulation models for cylindrical and toridal plasma, J. Comput. Phys. 25, 133, 1977a.

Cheng, C. Z., and H. Okuda, Formation of convective cells, anomalous diffusion and strong plasma turbulence due to drift instabilities, Phys. Rev. Lett. 38, 708, 1977b.

Cheng, C. Z., and H. Okuda, Theory and numerical simulations on collisionless drift instabilities in three dimensions, Nucl. Fusion 18, 587, 1978a.

Cheng, C. Z., and H. Okuda, Numerical simulation of trapped electron instabilities in toroidal geometry, Phys. Rev. Lett. 41, 1116, 1978b.

Cheng, C. Z., and C. S. Lin, Eigenmode analysis of compressional Alfvén waves in the magnetosphere, Geophys. Res. Lett., 14, 884, 1987.

Cheng, C. Z., and C. S. Lin, Theory of low-frequency Alfvén waves, EOS 69, 1384, 1988.

Cheng, C. Z., Kinetic extensions of magnetohydrodynamic models for axisymmetric toroidal Plasmas, Princeton Plasma Physics Laboratory Report, PPPL-2604, 1989.

Cheng, C. Z., Alpha particle effects on low-n magnetohydrodynamic modes, Fusion Technology 18, 443, 1990a.

Cheng, C. Z., Energetic particle effects on global magnetohydrodynamic modes, Phys. Fluids B2, 1427, 1990b.

Cheng, C. Z., K. Takahashi, and A. T. Y. Lui, Drift mirror and ballooning instabilities in the magnetosphere, EOS 71, 925, 1990.

Cheng, C. Z., Alpha particle destabilization of toroidicity-induced Alfvén eigenmode, Princeton Plasma Physics Laboratory Report PPPL-2717, to appear in Phys. Fluids B, 1991a.

Cheng, C. Z., Magnetospheric equilibrium with anisotropic pressure, Princeton Plasma Physics Laboratory Report PPPL-2762, submitted to J. Geophys. Res., 1991b.

Cummings, W. D., R. J. O'Sullivan, and P. J. Coleman, Jr., Standing Alfvén waves in the magnetosphere, J. Geophys. Res. 74, 778, 1969.

Frieman, E. A., and L. Chen, Nonlinear gyrokinetic equation for low-frequency electromagnetic waves in general plasma equilibria, Phys. Fluids 25, 502, 1982.

Grad, H., in Magneto-Fluid and Plasma Dynamics, Symposia in Applied Mathematics (Am. Math. Soc.), 18, 162, 1967.

Hahm, T. S., Nonlinear gyrokinetic equations for tokamak microturbulence, Phys. Fluids 31, 2670, 1988.

Hasegawa, A., Drift mirror instability in the magnetosphere, Phys. Fluids 12, 2642, 1969.

Lee, W. W., Gyrokinetic particle simulation model, J. Comput. Phys. 72, 243, 1987.

Morse, P. M., and H. Feshbach, in Methods of Theoretical Physics, McGraw-Hill Book Company, Inc., p. 467, 1953.

Pokhotelov, O. A., V. A. Pilipenko, Yu. M. Nezlina, J. Woch, G. Kremser, A. Korth, and E. Amata, Excitation of high-β plasma instabilities at the geostationary orbit; theory and observations, Planet. Space Sci. 34, 695, 1986.

Radoski, H. R., Magnetic toroidal resonances and vibrating field lines, J. Geophys. Res. 71, 1891, 1966.

Rutherford, P. H., and E. A. Frieman, Drift instabilities in general magnetic field configurations, Phys. Fluids 11, 569, 1968.

Southwood, D. J., Some features of field line resonances in the magnetosphere, Planet. Space Sci. 22, 483, 1974.

Southwood, D. J., A general approach to low-frequency instability in the ring current plasma, J. Geophys. Res. 81, 3340, 1976.

Southwood, D. J., and M. G. Kivelson, Charged particle behaviour in low-ffrequency geomagnetic pulsations: 2. Graphical approach, J. Geophys. Res., 87, 1707, 1982.

Takahashi, K., J. F. Fennell, E. Amata, and F. R. Higbie, Field-aligned structure of the storm time Pc 5 wave of November 14-15, 1979, J. Geophys. Res. 92, 5857, 1987.

Takahashi, K., Multisatellite studies of ULF waves, Adv. Space Res. 8, 427, 1988.

Takahashi, K., C. Z. Cheng, R. W. McEntire, T. A. Potemra, and L. M. Kistler, Observation and theory of compressional Pc 5 waves with second-harmonic component, J. Geophys. Res. 95, 977, 1990.

Tataronis, J., and W. Grossmann, Decay of MHD waves by phase mixing I. The sheet pinch in plane geometry, Z. Phys. 261, 203, 1973.

Taylor, J. B., and R. J. Hastie, Stability of general plasma equilibria I. Formal theory, Plasma Phys. 10, 479, 1968.

Tsang, K. T., and C. Z. Cheng, Gyrokinetic simulation of microinstabilities in high temperature tokamaks, Phys. Fluids B3, 688, 1991.